A structural study of deeply supercooled water

1989 J. Phys.: Condens. Matter 1 7123

(http://iopscience.iop.org/0953-8984/1/39/024)

J. Phys.: Condens. Matter **1** (1989) 7123–7129. Printed in the UK

A structural study of deeply supercooled water

M-C Bellissent-Funel†, J Teixeira†, L Bosio‡ and J C Dore§

† Laboratoire Léon Brillouin‖, CEN-Saclay, 91191 Gif-sur-Yvette Cédex, France

‡ Laboratoire de Physique des Liquides et Electrochimie du CNRS, ESPCI, 10 rue Vauquelin, 75231 Paris Cédex 05, France

§ Physics Laboratory, University of Kent, Canterbury, Kent CT2 7NR, UK

Received 22 February 1989, in final form 25 April 1989

Abstract. A new structural investigation of deeply supercooled water has been performed by neutron diffraction, down to −31.5 °C, using emulsions constituted by a mixture of deuteroheptane and CCl_4 with sorbitan as surfactant. The pair distribution function of water shows an increase of the spatial correlations which confirms the fact that the structure of deeply supercooled water tends towards that of low-density amorphous ice.

1. Introduction

The local order of deeply supercooled water has already been investigated down to −29 °C [1]. The previous results showed that the diffraction pattern obtained at −29 °C exhibited some features characteristic of amorphous ice. In this paper, we report on a new structural investigation in the deeply supercooled state, from −10.5 °C to −31.5 °C.

In the preceding experiment [1] we showed the temperature dependence of the structure factor which appears to indicate an evolution towards the structure of amorphous ice. In this paper, we extend the measurements down to −31.5 °C (typically, the supercooling limit compatible with our measuring time) and give a more complete analysis of the pair-correlation function.

2. Theory

The basic theory for studies of neutron scattering from molecular systems is well known and only the essentials will be repeated here.

The liquid structure factor $S_M(Q)$ can be written in terms of a molecular form factor $f_1(Q)$ and a difference function $D_M(Q)$ which contains all the intermolecular contributions, i.e.

$$S_M(Q) = f_1(Q) + D_M(Q). \tag{1}$$

For D_2O molecules, $f_1(Q)$ is given by

$$f_1(Q) = [b_O^2 + 2b_D^2 + 4b_O b_D j_0(Qr_{OD}) \exp(-\gamma_{OD}Q^2) + 2b_D^2 j_0(Qr_{DD}) \exp(-\gamma_{DD}Q^2)]/(b_O + 2b_D)^2 \tag{2}$$

‖ Laboratoire commun CEA–CNRS.

0953-8984/89/397123 + 07 $02.50

where r_{OD} is the intramolecular oxygen–deuterium distance and $r_{DD} = 2r_{OD}\sin(\frac{1}{2}\beta)$ for an intramolecular bond angle β, $j_0(x) = (\sin x/x)$ and $\gamma_{ij} = \frac{1}{2}\langle u_{ij}^2\rangle$ where $\langle u_{ij}^2\rangle$ is the mean-square amplitude of the displacement from the equilibrium position due to the normal mode vibration of the molecule. b_O and b_D are the coherent scattering lengths of oxygen and deuterium atoms ($b_O = 0.5805 \times 10^{-12}$ cm, $b_D = 0.6674 \times 10^{-12}$ cm).

The total pair-correlation function $g(r)$ is related to the Fourier transform of $S_M(Q)$ by

$$d(r) = 4\pi r\rho_M[g(r) - 1] = \frac{2}{\pi}\int_0^\infty Q[S_M(Q) - S_M(\infty)]\sin Q\,r\,\mathrm{d}Q \tag{3}$$

where $S_M(\infty) = (b_O^2 + 2b_D^2)/(b_O + 2b_D)^2$ is the asymptotic value of $f_1(Q)$ at large Q and ρ_M is the molecular number density.

The function $d(r)$ is a combination of the separate partial correlation functions and includes sharp peaks due to the intramolecular distances. It is more convenient to remove the intramolecular terms by subtracting the molecular form factor from $S_M(Q)$ to give $D_M(Q)$, which may be transformed by

$$d_L(r) = 4\pi r\rho_M[g_L(r) - 1] = \frac{2}{\pi}\int_0^\infty QD_M(Q)\sin Q\,r\,\mathrm{d}Q \tag{4}$$

to give the pair-correlation functions $d_L(r)$ and $g_L(r)$ for the intermolecular terms only.

The composite function $g_L(r)$ (or $d_L(r)$) consists of a weighted sum of partial terms which for neutron diffraction by D_2O is expressed by

$$g_L(r) = 0.489g_{DD}(r) + 0.421g_{OD}(r) + 0.090g_{OO}(r) \tag{5}$$

where the dominant contributions concern the D–D and O–D spatial correlations.

3. Experimental procedure and sample preparation

The experiments have been performed at the reactor Orphée at Saclay, on the 7C2 spectrometer [2] which is equipped with a BF_3 position sensitive detector with 640 cells; the angular step between two adjacent cells is equal to 0.2 degrees which leads to a maximum diffraction angle 2θ of 128 deg. The wavelength used ($\lambda = 0.707$ Å) allowed us to cover a scattering-vector ($Q = 4\pi(\sin\theta)/\lambda$) range extending from 0.3 $Å^{-1}$ to 16 $Å^{-1}$.

We increased the degree of supercooling of water by using emulsions constituted with a mixture of deuteroheptane and CCl_4, with sorbitan as surfactant; the average size of the water droplets was around a few μm. According to the measurements of the nucleation rate of ice in supercooled water by Taborek [3], the composition of the mixture has been chosen such as its density is close to that of water. If the density difference between the mixture and the pure water is too large, the instability of the emulsion is increased and a rapid phase separation occurs. A suitable composition is obtained by an equal mixture (by volume) of C_6D_{12} and CCl_4 with a small amount of sorbitan. The emulsion is then made by adding an equal volume of D_2O to this mixture such that the volume fraction, α_V (D_2O/emulsion) is 0.50. The precise composition of the emulsion used was 1 cm^3 of C_6D_{12}, 1 cm^3 of CCl_4, 2 cm^3 of D_2O and 80 mg of sorbitan.

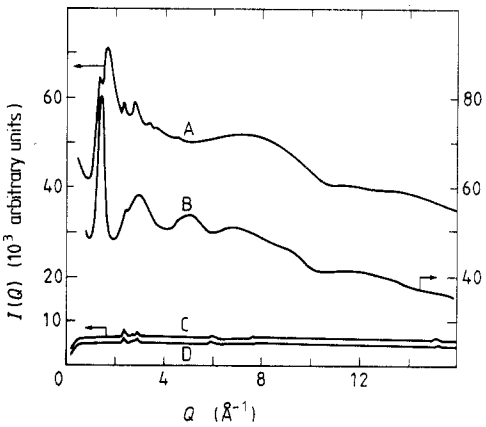

Figure 1. Experimental neutron scattering curves done in a cryostat, at −31.5 °C. Curve A, emulsion in a vanadium container; curve B, oil–surfactant mixture in a vanadium container; curve C, empty vanadium container; curve D, empty cryostat.

The samples were placed in an 8 mm diameter vanadium container, inside a helium cryostat. For a given temperature, several runs were performed successively. The acquisition time of each run was short in order to check frequently for eventual crystallisation of the sample. At the end all the runs were added together. We also measured the scattering due to background (empty cryostat), empty vanadium container and that of the oil–surfactant mixture necessary for the data analysis.

In figure 1, the raw data relative to the empty cryostat, to the empty vanadium cell in the cryostat, and to the sample at −31.5 °C (both emulsion and mixture) are plotted versus the wavevector Q.

4. Data analysis

The first step in the analysis was to correct the samples for background and absorption effects, using the classical Paalman and Pings procedure [4], with the calculated values of the total (absorption + scattering) linear coefficients, μ_T^E and μ_T^M relative respectively to the emulsion and to the oil-surfactant mixture ($\mu_T^E = 0.695\ \text{cm}^{-1}$, $\mu_T^M = 0.72\ \text{cm}^{-1}$ at room temperature). Multiple scattering corrections have also been applied to both the emulsion and the oil–surfactant mixture at each temperature, using a method described in [5].

A second step in the analysis was to eliminate the contribution due to the oil–surfactant mixture, in order to recover the water contribution. In the pattern of the emulsion, the contributions to the scattered intensity include several terms. Among the terms relative to the water, the oil–water and surfactant–water terms need to be examined. Due to the very low quantity of surfactant, we can neglect the surfactant–water contribution. The oil–water contribution concerns correlations between the molecules in a layer of oil–surfactant mixture and the water molecules at the surface of the water droplets which have an average diameter around 1 μm. Due to the large size of the water droplets, we assume that the oil–water contributions are negligible.

The water contribution $I^W(Q)$ can then be written as

$$I^W(Q) = I^E(Q) - \alpha I^M(Q) \tag{6}$$

where $I^E(Q)$ and $I^M(Q)$ refer to the emulsion and oil–surfactant mixture, respectively, and α is a coefficient depending on the composition of the emulsion as defined previously.

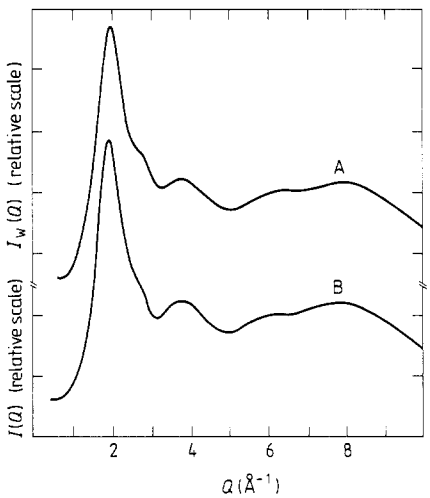

Figure 2. Spectrum $I^W(Q)$ of D_2O obtained at −10.5 °C (curve A) compared with spectrum $I(Q)$ of the bulk D_2O at −10.5 °C (curve B) [6].

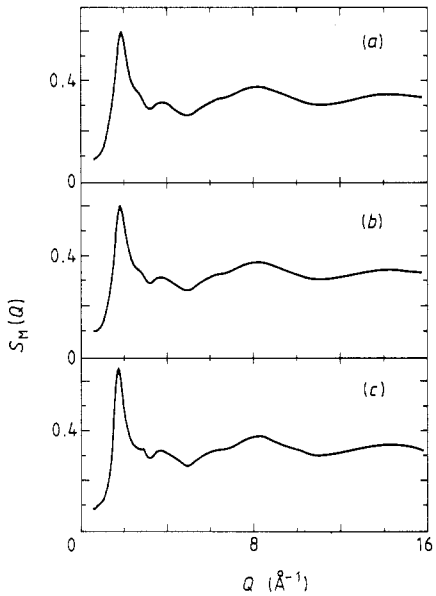

Figure 3. Structure factors $S_M(Q)$ of D_2O obtained at (*a*) −10.5 °C, (*b*) −18.5 °C and (*c*) −31.5 °C.

We determined experimentally the value of α, comparing the results obtained for water in the emulsion at −10.5 °C, with those obtained with bulk water at almost the same temperature [6]. The best agreement corresponds to $\alpha = 0.55 \pm 0.01$.

In figure 2, the spectrum $I^W(Q)$ of water at −10.5 °C is plotted against Q, and compared with that of the bulk sample. A good agreement is observed between both spectra. This comparison allowed us to check the validity of the correction procedure involving subtraction of the scattering by the oil phase.

After the usual absorption and multiple scattering corrections and the elimination of the oil–surfactant mixture contribution, we obtain, (from (6)), a spectrum $I^W(Q)$ which contains both $S_M(Q)$ and the incoherent scattering contribution in an arbitrary scale, together with the inelasticity effects. The complete evaluation of inelasticity corrections for water is complex and in some respects remains controversial but here we use an empirical method, already applied with success to the data analysis of high-density amorphous ice [7] and recently to the determination of a single $S_M(Q)$ of liquid water from experiments at three different wavelengths [8].

5. Discussion and comparison with amorphous ice

5.1. *Interference functions $S_M(Q)$ and $D_M(Q)$*

In figure 3, the derived structure factors $S_M(Q)$ are plotted versus Q, at −10.5 °C, −18.5 °C and −31.5 °C. We observed a temperature dependence of $S_M(Q)$ characterised by a displacement of the main diffraction peak position Q_0 towards smaller Q values with decreasing temperature as observed in previous experiments [9]. The evolution of

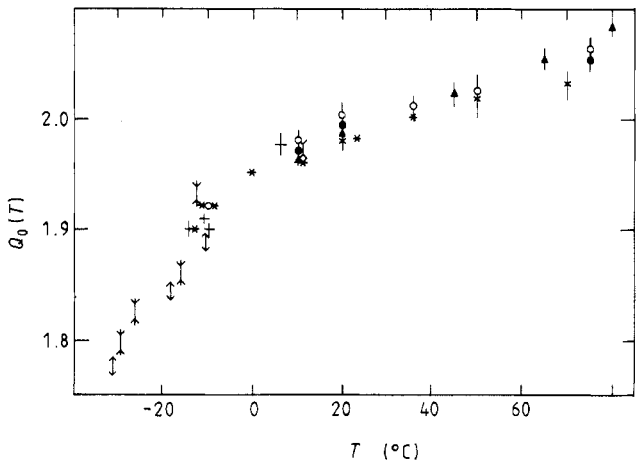

Figure 4. Evolution of the main neutron diffraction peak $Q_0(T)$ of $S_M(Q)$ versus temperature. ↕, this work. For the other symbols, see [1].

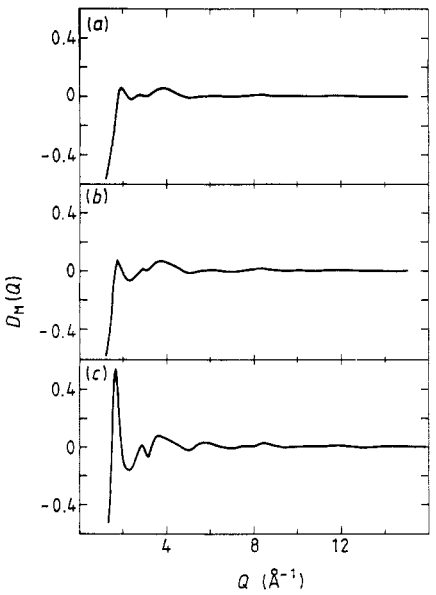

Figure 5. Intermolecular functions $D_M(Q)$ of D_2O obtained at (*a*) −10.5 °C and (*b*) −31.5 °C. (*c*) The function $D_M(Q)$ of low-density amorphous ice given for comparison [10].

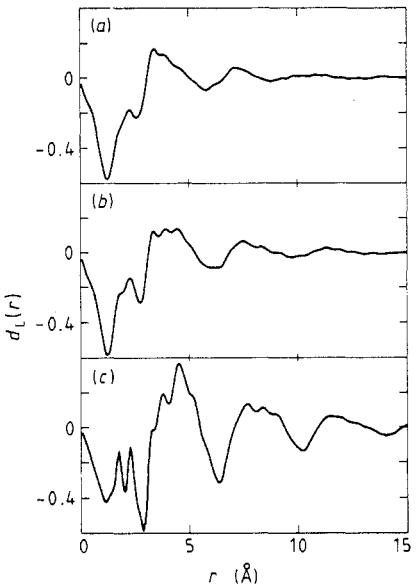

Figure 6. Pair-correlation functions $d_L(r)$ of D_2O obtained at (*a*) −10.5 °C and (*b*) −31.5 °C. (*c*) The function $d_L(r)$ of low-density amorphous ice given for comparison [10].

Q_0 as a function of temperature is given in figure 4. It appears that Q_0 tends towards the value 1.7 Å^{-1} which is characteristic of low-density amorphous ice. Moreover, the slope of the $Q_0(T)$ function increases with decreasing temperature. The slope of $Q_0(T)$ in the lower temperature regions correlates with the decrease in bulk density and emphasises the link between the microscopic and macroscopic features. The extrapolations of both density and $Q_0(T)$ curves below the lowest temperatures for which data are available give the corresponding values for amorphous ice in a region around −40 °C. However, in our opinion these temperatures have no particular signification. In figure 5 the

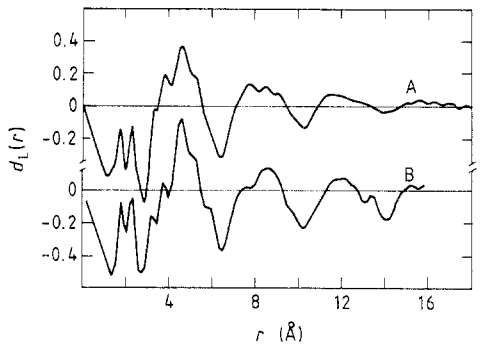

Figure 7. Comparison between the experimental $d_L(r)$ of low-density amorphous D_2O ice (curve A) and that obtained from the continuous random network (CRN) model [12] (curve B).

intermolecular functions $D_M(Q)$ are plotted versus Q, at −10.5 °C and −31.5 °C together with that of low-density amorphous ice.

5.2. Pair-correlation functions d_L(r)

In figure 6, the pair-correlation function of amorphous ice [10] is plotted, together with that of supercooled water, at −10.5 °C and at −31.5 °C.

In the small-r range, when the temperature is lowered, some features characteristic of amorphous ice show up: for example, two peaks appear at 1.75 Å and 2.30 Å the first one corresponding to the hydrogen-bond distance and the second one to the intermolecular D–D distance. In the large-r range one observes additional small oscillations, which are not present at −10.5 °C and an out of phase behaviour for the broad oscillations ($r > 10$ Å). These features are similar to those observed in low-density amorphous ice. Neutron diffraction is sensitive to both position and angular correlations and $d_L(r)$ is dominated by the partial functions $g_{OD}(r)$ and $g_{DD}(r)$ (see equation (5)). Because x-ray data show that oxygen–oxygen distances are not strongly temperature dependent [9], the observed strong temperature evolution of $g(r)$ is mainly due to the temperature dependence of the g_{OD} and g_{DD} pair-correlation functions. The increased effect of hydrogen-bonding therefore produces enhanced orientational correlations between neighbouring molecules and, as the hydrogen-bonded clusters increase in size, there is a greater spatial correlation between second- and third-bonded molecules. However, the assembly still possesses liquid characteristics so that the correlations of the transient hydrogen-bonded assemblies are less developed than in the static structure of amorphous ice.

5.3. Comparison with amorphous ice

In order to interpret the behaviour of the pair correlation function of water at −31.5 °C, we recall that an appropriate description of the structure of amorphous ice has been given in terms of a continuous random network (CRN) model [10]. In this model, the basic building unit is a water pentamer. This is equivalent to a description of the molecular arrangement in water by a continuous random network of tetrahedrally-coordinated H-bonds [11].

Figure 7 gives the comparison between the experimental $d_L(r)$ [10] and the theoretical one [12] for the amorphous ice. A good agreement is observed, at least at small and medium r.

Further support for this viewpoint is provided from some recent neutron diffraction experiments on hyperquenched solid water [13] where it is shown that rapid cooling of liquid droplets in a supersonic jet produces a form of vitreous ice which has a very similar structure to that of vapour-deposited amorphous ice. The fully hydrogen-bonded network is therefore a natural end product of the structural evolution of the system with decreasing temperature if crystallisation can be suppressed.

6. Conclusion

The present results confirm the increasing spatial correlations in deeply supercooled liquid water as the temperature is decreased. These new data should provide an important basis for a comparison with predictions based on different forms of the interaction potential between water molecules. Earlier work on simulations for water under ambient conditions appeared to give too much structure to the $g(r)$ functions and insufficient variation with temperature. It can now be appreciated that the essential geometrical features which are influenced by the tetrahedral nature of the hydrogen-bonding are manifest only in the lower temperature regime. The structural information will therefore be much more sensitive to parameters defining the potential and could possibly lead to the resolution of the long-standing controversy over whether a two-body interaction is adequate for the description of liquid water.

References

[1] Bellissent-Funel M-C, Bosio L, Dore J C, Teixeira J and Chieux P 1986 *Europhys. Lett.* **2** 241
[2] Ambroise J-P, Bellissent-Funel M-C and Bellissent R 1984 *Phys. Rev. Appl.* **19** 731
[3] Taborek P 1985 *Phys. Rev.* B **32** 5902
[4] Paalman H H and Pings C J 1962 *J. Appl. Phys.* **39** 2635
[5] Menelle A 1987 *Thesis* Université Paris VI
[6] Sufi M A M, Dore J C, Teixeira J, Bellissent-Funel M-C, Bosio L and Chieux P in preparation
[7] Bellissent-Funel M-C, Teixeira J and Bosio L 1987 *J. Chem. Phys.* **87** 2231
[8] Bellissent-Funel M-C, Teixeira J, Bosio L and Dore J C in preparation
[9] Bosio L, Teixeira J, Dore J C, Steytler J and Chieux P 1983 *Mol. Phys.* **50** 733
[10] Chowdhury M R, Dore J C and Wenzel J T 1982 *J. Non-Cryst. Solids* **53** 247
[11] Geiger A, Stillinger F H and Rahman A 1979 *J. Chem. Phys.* **70** 4185
Stanley H E and Teixeira J 1980 *J. Chem. Phys.* **73** 3404
[12] Boutron P and Alben R 1975 *J. Chem. Phys.* **62** 4848
Sceats M G, Stavola M and Rice S A 1979 *J. Chem. Phys.* **70** 3927
[13] Halbrucker A, Mayer E, O'Mard L, Dore J C and Chieux P in preparation